

Supplementary Figure 1. Tc9 cells have lower ROS production and similar ROS scavenging ability compared to Tc1 cells.

(A) Survival condition of Tc1 or Tc9 cells treated mice (n = 7). (B) Polarized Tc1 and Tc9 cells were treated with TBH (100 μ M) and then washed with PBS. Cellular ROS levels were detected and ROS scavenging rates [(ROS level at 0.5 hour - ROS level at 1.5 hours) / Time] are shown (n = 3). (C) Polarized Tc1 and Tc9 cells were treated with N-Acetyl Cysteine (NAC, 50 μ M) and then washed with PBS. Cellular ROS levels were detected and ROS production rates [(ROS level at 17 hour - ROS level at 1 hour) / Time] are shown (n = 3). Data are presented as mean \pm SEM. *p < 0.05; ***p < 0.001 with log-rank (Mantel–Cox) test in A and unpaired 2-tailed Student's *t* test in other panels.

Supplementary Figure 2. Persistence of adoptively transferred CD8⁺ T cells in TME is negatively correlated with their lipid peroxidation.

(A) Tumor-infiltrating Tc1 or Tc9 cells were divided into PD-1⁺ and PD-1⁻ groups and analyzed for the ratio of PD-1⁺ and PD-1⁻ (n = 10). (B) GSEA of exhaustion associated gene enrichment in tumor-infiltrating Tc1 or Tc9 cells. (C-F) Thy1.1⁺ Pmel-1 Tc1 or Tc9 cells were i.v. injected into s.c. B16 tumor-bearing Thy1.2⁺ B6 mice with adjuvant treatments. Thy1.1⁺ percentages in CD8⁺ T cell and relative lipid ROS of Tc1 and Tc9 cells in peripheral blood and spleens (n = 8-10). (G-J) Thy1.1⁺ Pmel-1 Tc1 or Tc9 cells were i.v. injected into MC38-gp100 tumor-bearing Thy1.2⁺ B6 mice with adjuvant treatments. Tumor growth curve, Thy1.1⁺ percentages in CD8⁺ T cell, and relative lipid ROS of Tc1 and Tc9 in spleens (n = 6). (K-M) Thy1.1⁺ Pmel-1 Tc1 or Tc9 cells were i.v. injected into Thy1.2⁺ B6 mice bearing lung B16 tumors. Tumor foci in lung, Thy1.1⁺ CD8⁺ T cell percentages, and relative lipid ROS of Tc1 and Tc9 in spleens (n = 6). Data are presented as mean \pm SEM. *p < 0.05; **p < 0.01; ***p < 0.001 with unpaired 2-tailed Student's *t* test.

Supplementary Figure 3. Reduced lipid peroxidation and ferroptosis are required for the persistence of Tc1 and Tc9 cells in TME.

(A-C) Mouse CD8⁺ T cells were isolated from Pmel-1 Thy1.1⁺ B6 mice and polarized with Hgp100₂₅₋₃₃ peptide under corresponding conditions. Relative *Trf* and *Tfrc* mRNA expression, relative lipid ROS and iron level in Tc1 and Tc9 cells on day 4 of polarization. (D-E) Polarized mouse Tc1 and Tc9 cells were cultured with IL-2 for another 5 days and then re-stimulated with CD3/CD28 antibodies. Relative lipid ROS and cell death are shown. (F) Relative cell viability in polarized mouse Tc1 and Tc9 cells treated with Fin56 under indicated concentrations. (G-H) Relative lipid ROS and Thy1.1⁺ percentages in CD8⁺ T cell from peripheral blood of indicate treated Tc9 cells as Figure 2J (n = 5). (I-J) Thy1.1⁺ Pmel-1 Tc1 cells treated with RSL3 (0.05 μM) or Fer-1 (5 μM) were injected into B16 tumor-bearing Thy1.2⁺ B6 mice with adjuvant treatments. Relative lipid ROS, Thy1.1⁺ percentages in CD8⁺ T and Thy1.1⁺ CD8⁺ T numbers of indicated Tc1 cells in tumor tissues on day 40 after tumor cell injection (n = 5). Data are presented as mean ± SEM. *p < 0.05; **p < 0.01. ***p < 0.001 with 1-way ANOVA followed by Dunnett's test in H, I, J, 2-way ANOVA in F and unpaired 2-tailed Student's *t* test in other panels.

Supplementary Figure 4. Positive correlation between ferroptosis and dysfunction in human melanoma CD8⁺ T cells.

(A) Kaplan–Meier analysis (log-rank test) of overall survival in *IL9* high or *IL9* low melanoma, colon cancer and breast cancer patients with high CD8⁺ infiltrates (see Method). (B-C) Melanoma patients' tumor-infiltrating CD8⁺ T cells were divided into dysfunctional and non-dysfunctional groups from previous study. GSEA and heatmap analyses of lipid peroxidation and ferroptosis activation-related genes in these different groups. (D-E) Melanoma patients were divided into non-responders and responders who received PD-1 or CTLA-4 checkpoint immunotherapy by analyzing previous data. GSEA and heatmap analyses of lipid peroxidation and ferroptosis activation-related genes in non-responders and responders.

Supplementary Figure 5. Tc9 cells display increased fatty acid oxidation activity compared to Tc1 cells.

(A-C) Relative lipid ROS, iron level, and relative cell viability in Tc1 and Tc9 treated with FFA or AA for 16 hours on day 4 of polarization (n = 6). (D) Heatmap analysis of fatty acid synthesis- and uptake- related genes in tumor-infiltrating Tc1 or Tc9 cells on day 14 after injection. (E-F) Relative mRNA expression of fatty acid β -oxidation-, synthesis- and uptake- related genes (n = 3). (G) Cpt1a expression in polarized Tc1 or Tc9 cells from WT mice on day 4 of polarization (n = 3). Data are presented as mean \pm SEM. *p < 0.05; ***p < 0.001 with 1-way ANOVA followed by Dunnett's test in A, B, C, and unpaired 2-tailed Student's *t* test in other panels.

Supplementary Figure 6. Increased fatty acid oxidation and mitochondrial activity are required for reduced lipid peroxidation and ferroptosis in Tc9 cells.

(A) MitoTracker intensity in polarized Tc1 and Tc9 cells (n = 6). (B-C) ECAR values at indicated treatments and basal OCR/ECAR ratio in Tc1 and Tc9 cells. (n = 6-8). (D) TMRM^{high} ratio and intensity in tumor-infiltrating Tc1 and Tc9 cells from s.c. B16 tumor-bearing mice (n=10). (E) TMRM intensity in Tc1 and Tc9 cells from spleens of s.c. B16 tumor-bearing mice (n=10). (F) CPT1A expression in scramble- and *Cpt1a* shRNA lentivirus-transduced Tc9 cells. or vector- and *Cpt1a* overexpressing (OE) retrovirus-transduced Tc9 cells in N (n = 2). (G) TMRM intensity, relative lipid ROS and cell viability in scramble shRNA- or Cpt1a shRNA lentivirus-transduced Tc9 cells treated with RSL3 (0.05 μ M) or TBH (60 μ M) for 16h. (H) CPT1A expression vector- and *Cpt1a* overexpressing (OE) retrovirus-transduced Tc9 cells (n = 2). FFA: free fatty acids, AA: arachidonic acid. Data are presented as mean \pm SEM. *p < 0.05; ***p < 0.001 with two-tailed unpaired *t* test.

Supplementary Figure 7. IL9/STAT3 signaling induces Cpt1a expression in Tc9 cells.

(A) IPA result of JAK/Stat pathway in tumor-infiltrating Tc1 and Tc9 cells on day 14 after injection. Red: upregulation. (B) Cpt1a expression in Stattic-treated Tc9 cells on day 4 of polarization. (C) p-STAT3 and Cpt1a expression in polarized Tc9 cells treated with IL-6 (30 nM) for 16 hours (n = 4). (D) Relative *Il6*, *Il10*, *Il27* and *Il9* mRNA expression in Tc1 and Tc9 cells on day 4 of polarization (n = 3). (E) IPA result of the crosstalk of STAT3 pathway and IL-9 signaling in tumor-infiltrating Tc9 cells. Data are presented as mean \pm SEM. *p < 0.05; ***p < 0.001 with 1-way ANOVA followed by Dunnett's test in B and unpaired 2-tailed Student's *t* test in other panels.

Supplementary Figure 8. IL-9 signaling up-regulates fatty acid oxidation to resist tumor or ROS induced ferroptosis in Tc9 cells.

(A) LC-MS analysis of indicated saturated, mono-unsaturated, and poly-unsaturated fatty acid contents in naïve CD8⁺ T cells isolated from WT or *Il9*^{-/-} mice before polarization (n=2). (B) Cpt1a expression in naïve CD8⁺ T cells in A (n=2). (C) LC-MS analysis of indicated saturated, mono-unsaturated, and poly-unsaturated fatty acid contents in polarized Tc1 or Tc9 from WT or *Il9*^{-/-} mice on day 4 of polarization (n=2). (D-G) TMRM intensity, cellular ROS level, relative lipid ROS, iron level and relative cell viability in polarized Tc9 cells from indicated mice treated with ROS inducer TBH for 16 hours (n = 3). (H-J) TMRM intensity, cellular ROS level, relative lipid ROS, iron level and relative cell viability in vector- or Cpt1a overexpression transduced Tc9 cells from indicated mice treated with ROS inducer TBH for 16 hours (n = 3). (K-M) TMRM intensity, cellular ROS level, relative lipid ROS, iron level and relative cell viability in vector- or Cpt1a overexpression transduced Tc9 cells from indicated mice after co-culture with B16 cells for 48 hours (n = 3). Data are presented as mean \pm SEM. *p < 0.05; **p < 0.01; ***p < 0.001 with 1-way ANOVA followed by Dunnett's test.

Figure 9. IL9 signaling deficiency dampens longevity of Tc9 cells in peripheral blood.

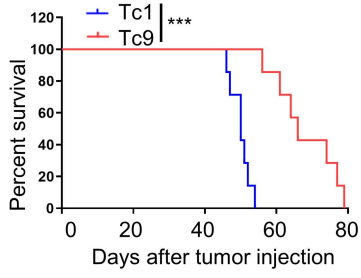
Thy1.1⁺ Pmel-1 Tc9 cells from Pmel-1-WT, *-Il9^{-/-}* and *-Il9r^{-/-}* mice were injected into Thy1.2⁺ B6 mice bearing 10-day s.c. B16 tumor as Figure 6A. **(A)** Relative lipid ROS, **(B)** iron level, **(C)** TMRM intensity, **(D)** Thy1.1⁺ percentages in CD8⁺ T cells of transferred T cells in peripheral blood (n = 5). Data are presented as mean ± SEM. *p < 0.05; **p < 0.01 with 1-way ANOVA followed by Dunnett's test.

Figure 10. Inhibiting STAT3-fatty acid oxidation pathway in Tc9 cells impairs their longevity in peripheral blood.

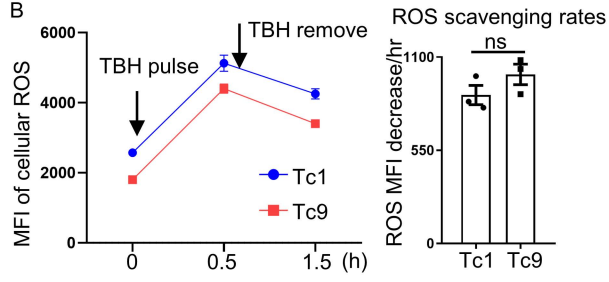
(A-E) Thy1.1⁺ Pmel-1 Tc9 cells were treated with DMSO (Ctrl), p-STAT3 inhibitor Stattic (0.5 μM), fatty acid oxidation inhibitor etomoxir (Eto, 50 μM), or ferroptosis inhibitor Fer-1 (5 μM) and then injected into Thy1.2⁺ B6 mice bearing 10-day s.c. B16 tumor as Figure 7A. Relative lipid ROS, iron level, TMRM intensity, Thy1.1⁺ percentages in CD8⁺ T cells of transferred T cells in peripheral blood (n = 5-6). **(F-H)** Thy1.1⁺ Pmel-1 Tc9 cells were overexpressed with vector or *Cpt1a* and injected into Thy1.2⁺ B6 mice bearing 10-day s.c. B16 tumor as Figure 7H. Relative lipid ROS, TMRM intensity, Thy1.1⁺ percentages in CD8⁺ T cells of transferred T cells in peripheral blood (n = 6). **(I-M)** Thy1.1⁺ Pmel-1 Tc1 or Tc9 cells from WT mice transduced with vector or *Cpt1a* were injected into B16 tumor bearing Thy1.2⁺ B6 mice with adjuvant treatments. Relative lipid ROS, TMRM intensity, Thy1.1⁺ percentages in CD8⁺ T cells and Thy1.1⁺ CD8⁺ T cells numbers, tumor growth curve, and the expression of PD-1 and LAG-3 on transferred CD8⁺ Thy1.1⁺ T cells in tumors (n = 5). **(N)** Schematic diagram shows that IL/9/STAT3/fatty acid oxidation mediated lower lipid peroxidation contributed to Tc9 cell longevity and enhanced antitumor activity. Eto: Etomoxir, OE: overexpressing. Data are presented as mean ± SEM. *p < 0.05; **p < 0.01; ***p < 0.001 with 1-way ANOVA followed by Dunnett's test in **A, B, E**, 1-way ANOVA followed by Turkey's test in **I, J, K, M**, 2-way ANOVA in **L** and unpaired 2-tailed Student's *t* test in other panels.

Supplementary Figure 1

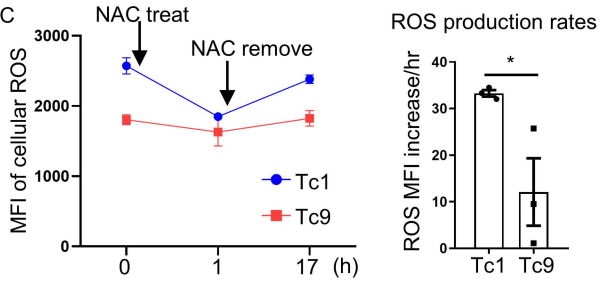
A



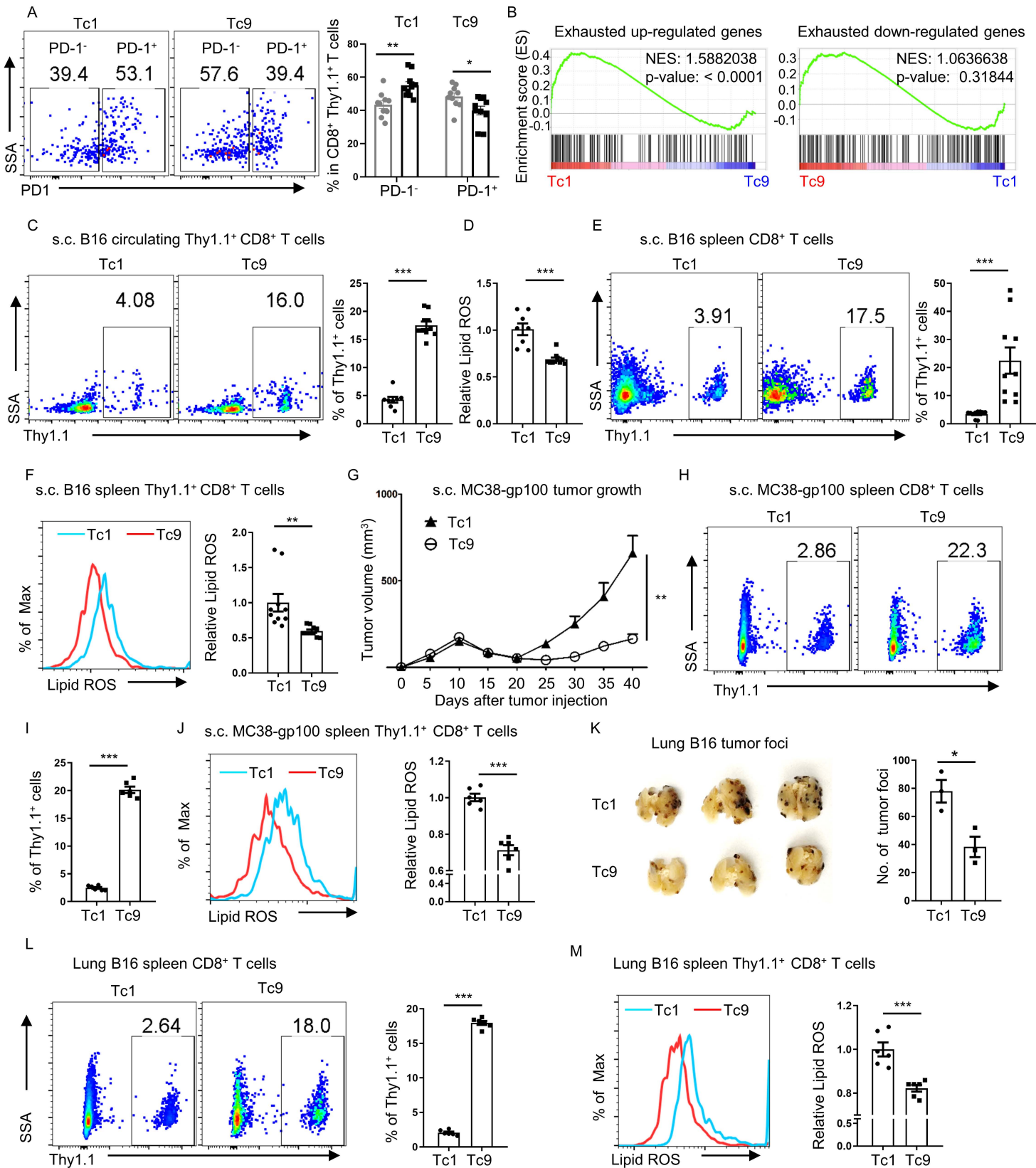
B



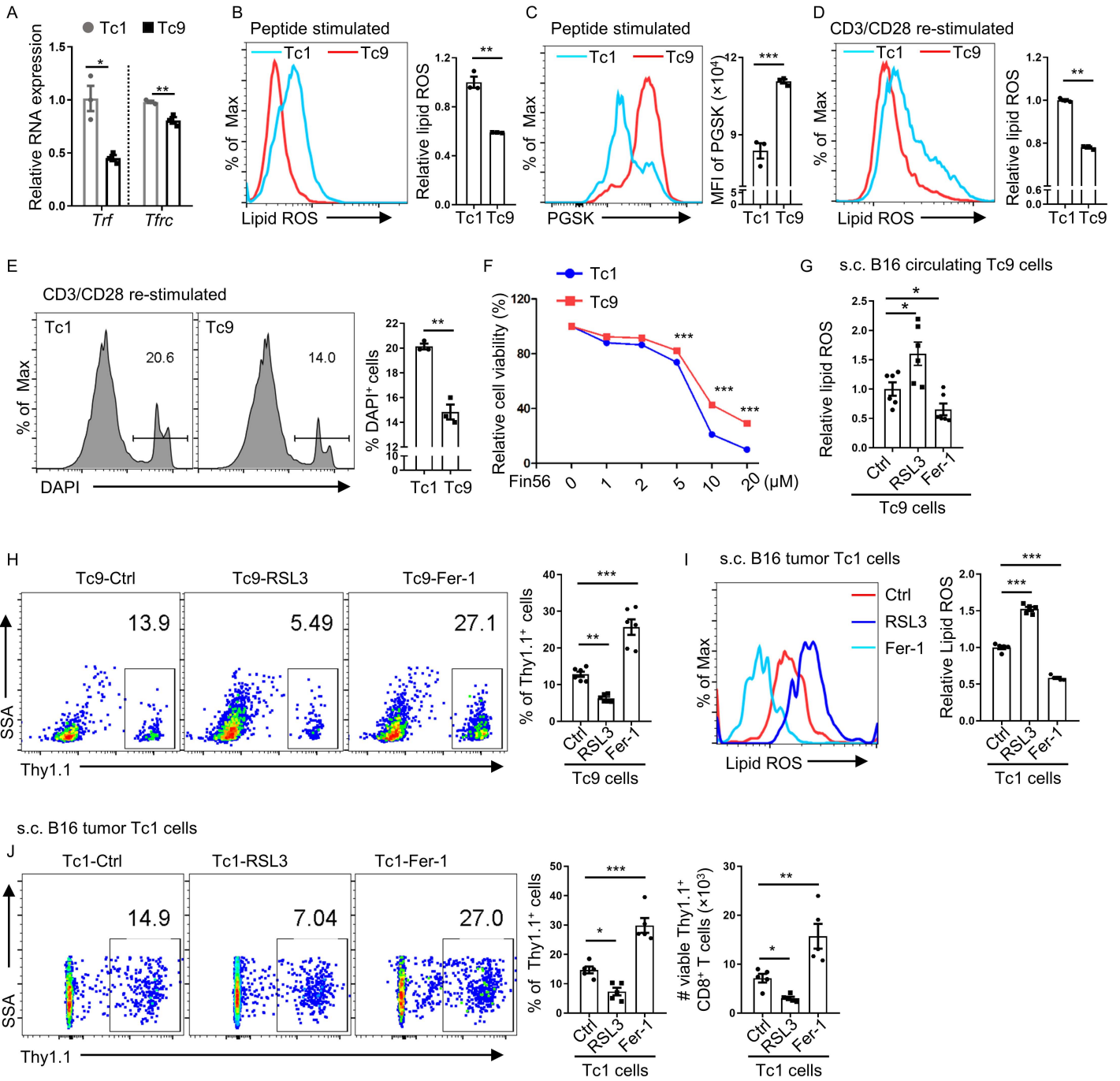
C



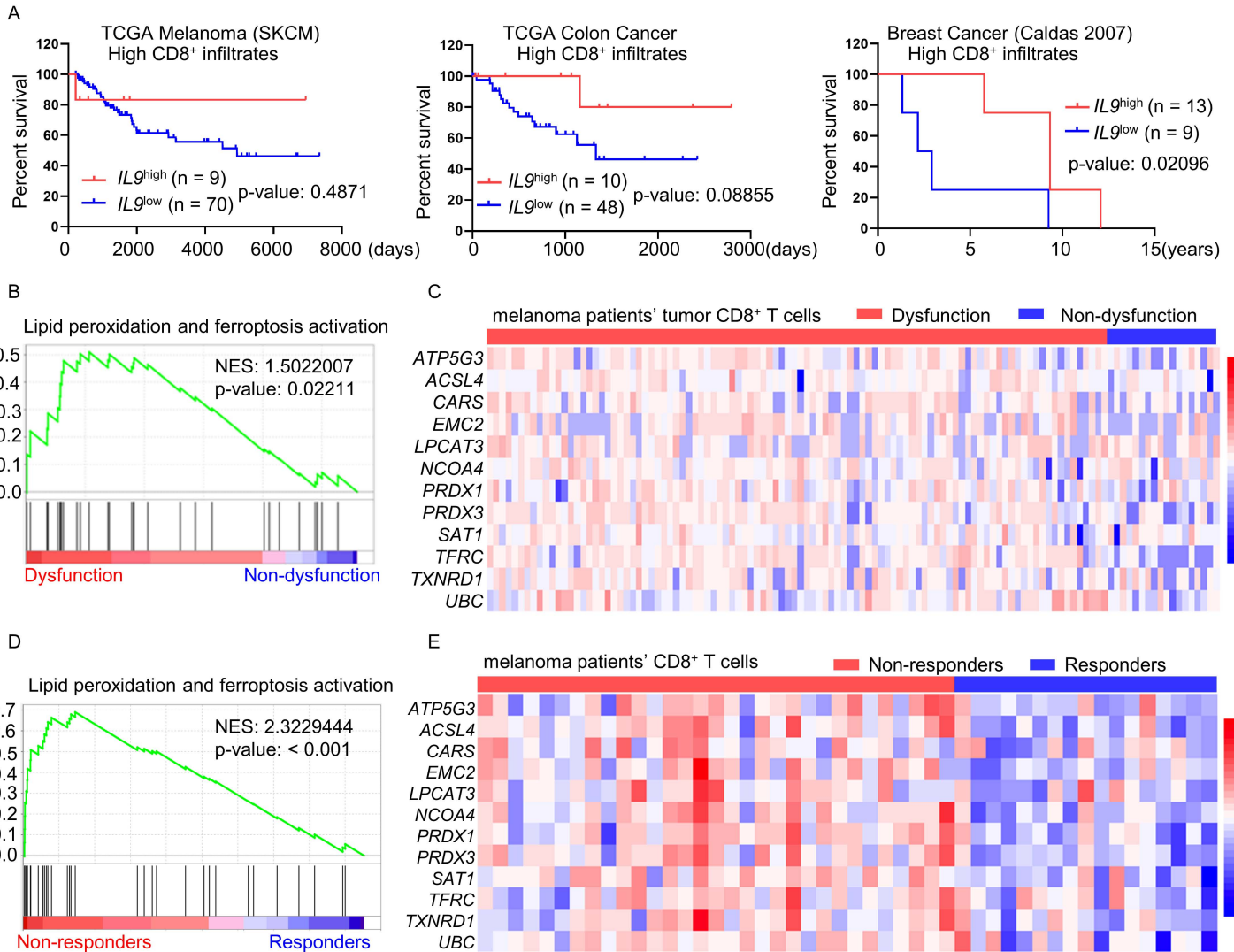
Supplementary Figure 2



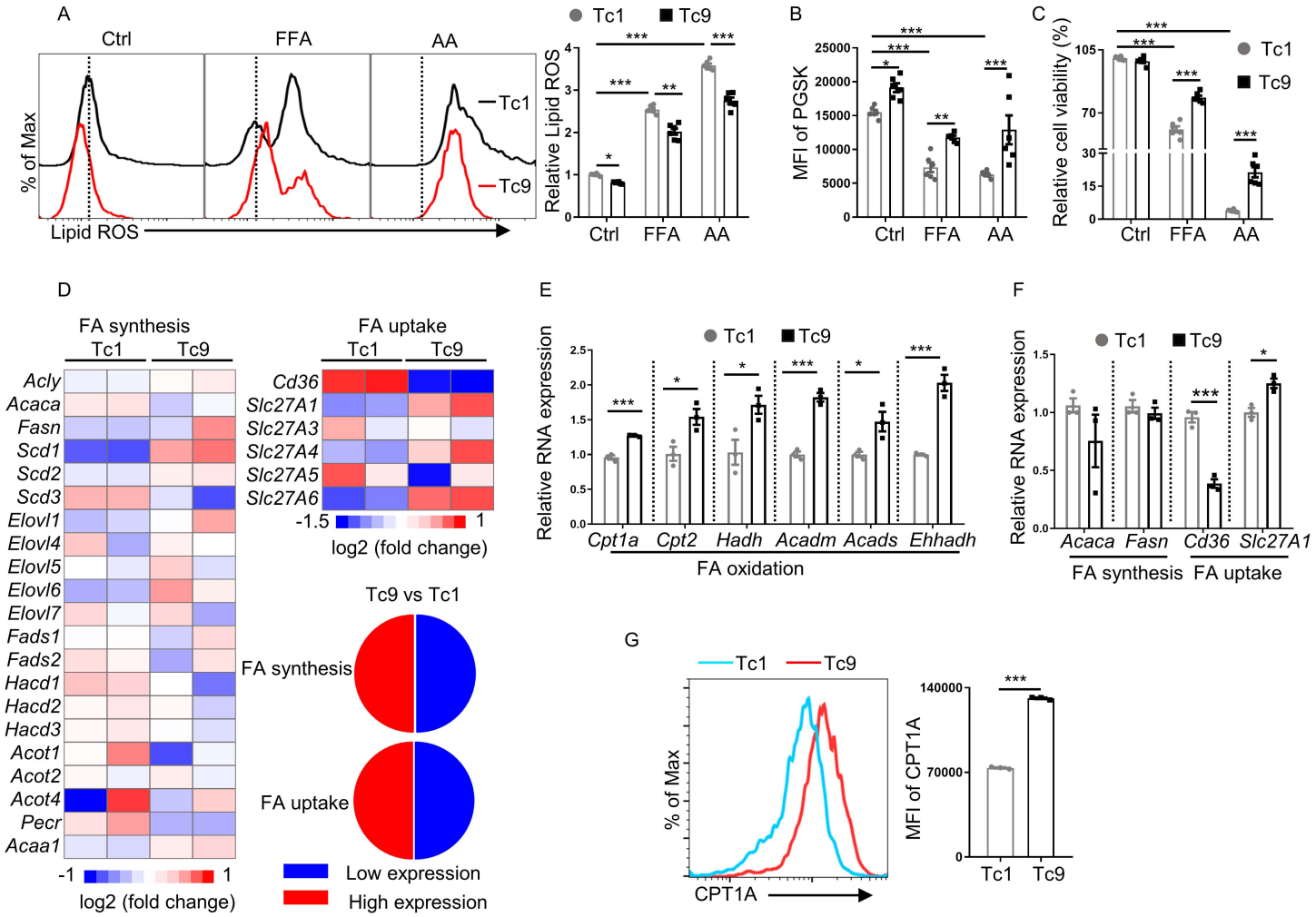
Supplementary Figure 3



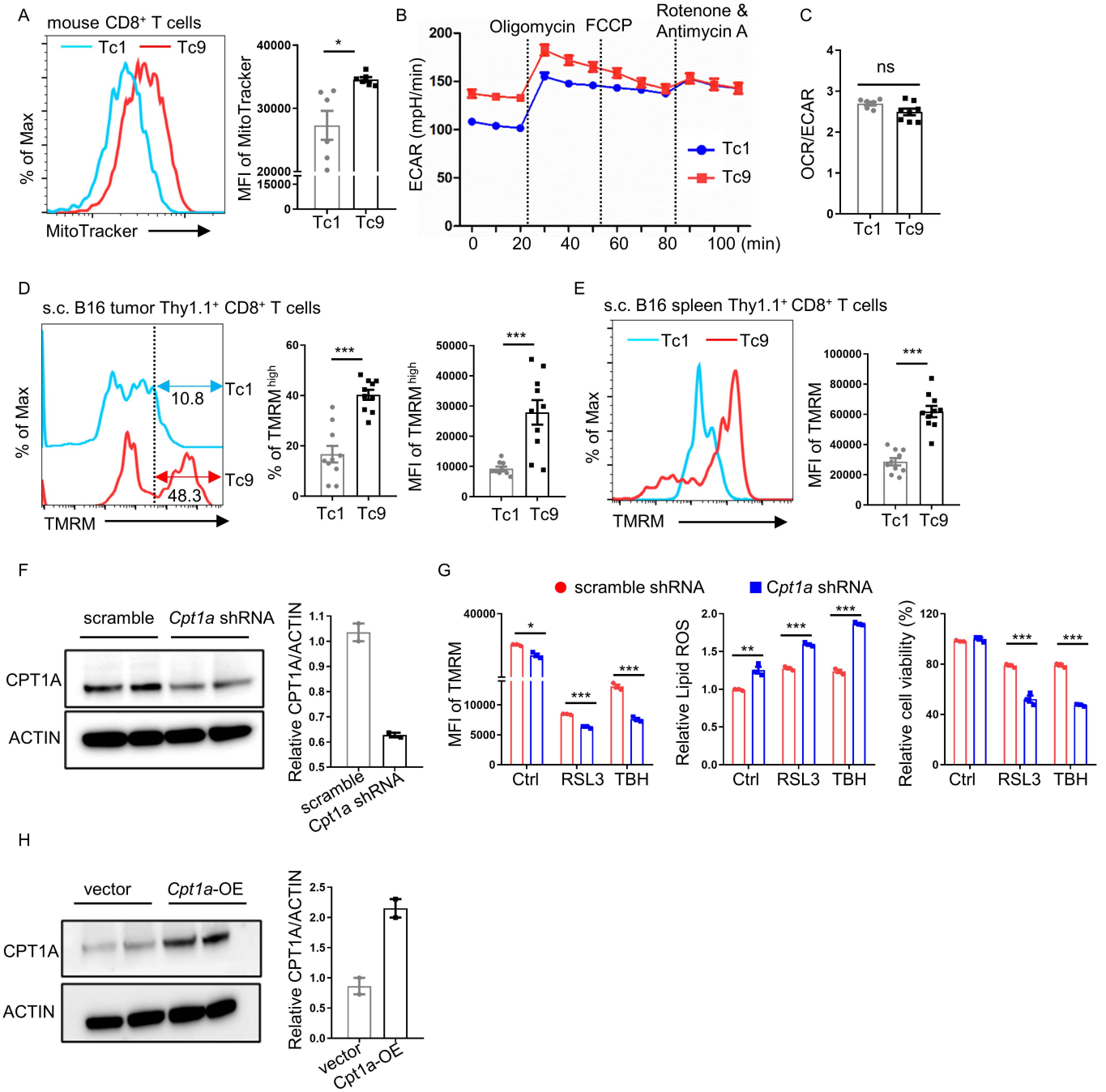
Supplementary Figure 4



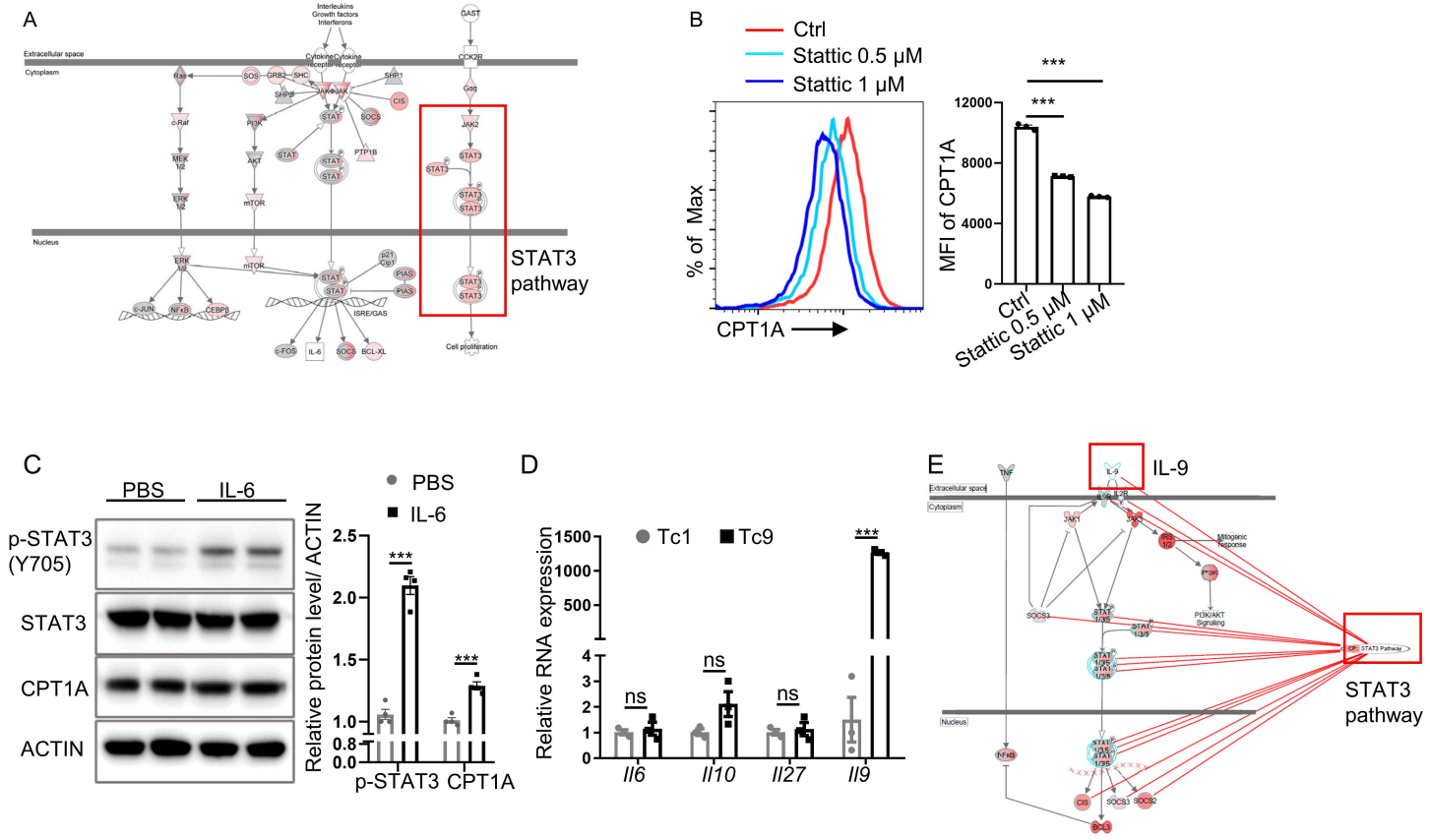
Supplementary Figure 5

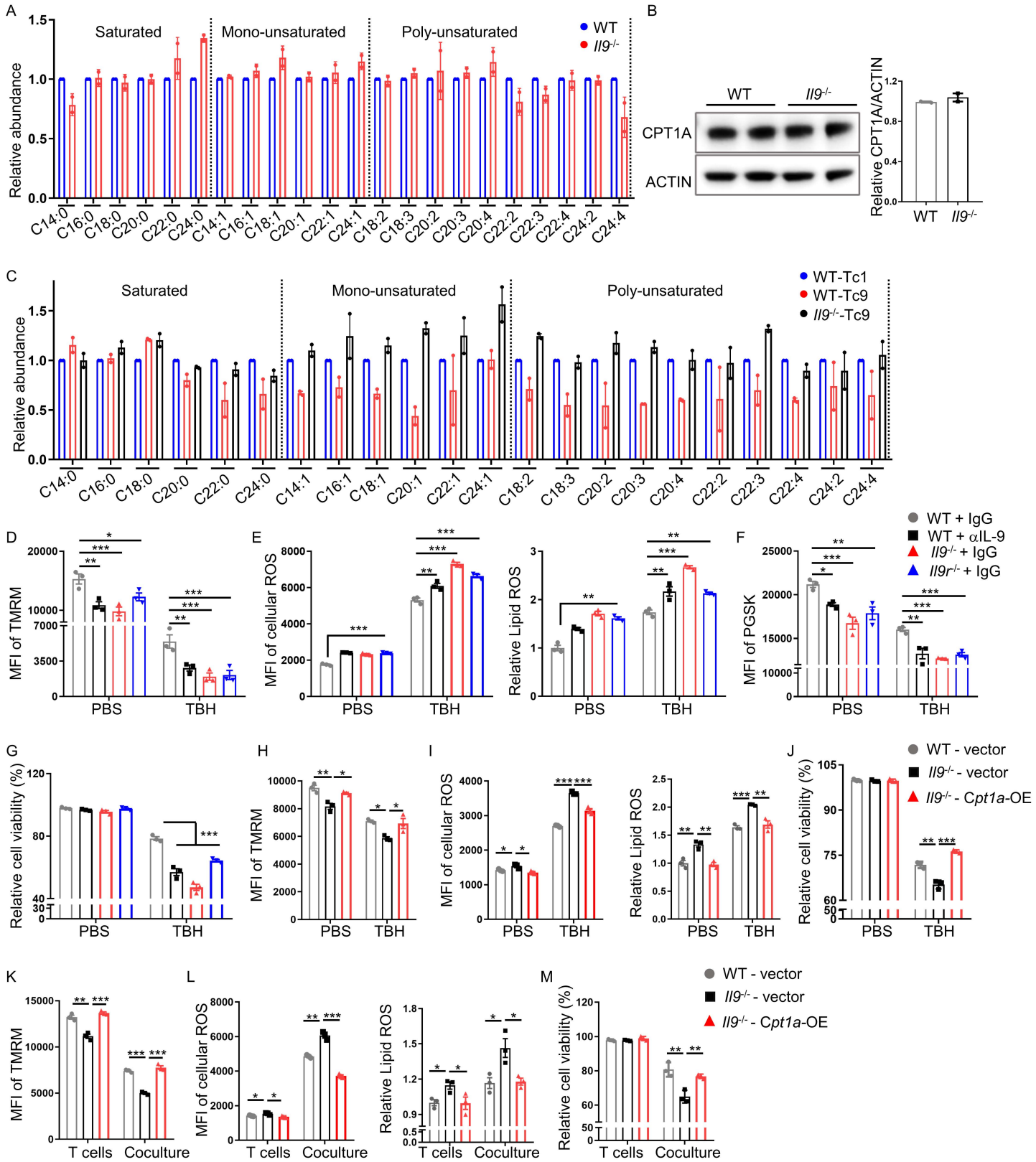


Supplementary Figure 6

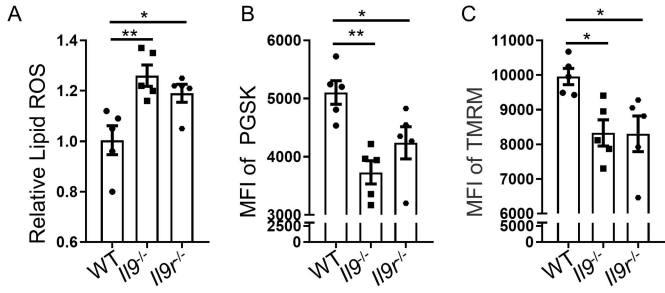


Supplementary Figure 7

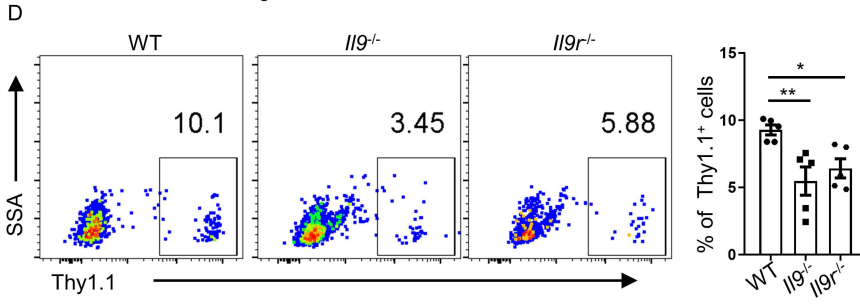




s.c. B16 circulating Thy1.1⁺ CD8⁺ T cells



s.c. B16 circulating CD8⁺ T cells



Supplementary Figure 10

s.c. B16 circulating Thy1.1⁺ CD8⁺ T cells

s.c. B16 circulating CD8⁺ T cells

